

Electronic Structure of Liquid Mercury Using Compton Scattering Technique

B. L. Ahuja, M. Sharma, and S. Mathur

Department of Physics, College of Science Campus, M. L. Sukhadia University, Udaipur 313001 (Raj.) India

Reprint requests to Dr. B. L. A.; E-mail: blahuja@yahoo.com

Z. Naturforsch. **59a**, 543 – 549 (2004); received April 10, 2004

The isotropic Compton profile of mercury has been measured, using 661.65 keV gamma-rays from a 20 Ci ^{137}Cs source. To extract the true experimental Compton line shape, besides the usual systematic corrections we have incorporated for the first time the background correction due to bremsstrahlung radiation generated by photo and Compton electrons. Theoretical computations have been carried out, using the renormalised-free-atom (RFA) for the electron configuration $4f^{14}5d^{10}6s^2$ and free electron models. It is found that the present experimental data with bremsstrahlung background correction are in better agreement with the RFA calculations. This work suggests the incorporation of the bremsstrahlung background correction in Compton scattering experiments of heavy materials using high-energy gamma-ray sources.

Key words: Electronic Structure; Compton Scattering; Electron Momentum Density; Mercury Metal.

1. Introduction

Mercury, which is liquid at room temperature, crystallizes at about -39°C to form a trigonal crystal. The structure of Hg can be regarded as distortion of an ideal fcc structure. It is a difficult task to handle and orient the soft single crystal well below the melting point. The electronic structure of liquid mercury is remarkably different from other metals. Considerable experimental and theoretical work has been done on Hg to determine its electronic band structure, Fermi surface and optical properties. An earlier review upto 1970 can be found in the work of Cracknell [1]. Among later work, several density of states calculations of liquid mercury (for a review, see [2]) have indicated the possibility of a pseudogap below the Fermi energy. Using *ab initio* density functional molecular dynamics simulation, Kresse and Hafner [3] have discussed a metal–nonmetal transition in expanded liquid Hg. This calculation was based on the k-space method, which uses unit cells of 50 atoms. To study the electronic properties, Jank and Hafner [4] have used the linear-muffin-tin orbital with atomic sphere approximation (LMTO-ASA), while Bose [5] has reported a scalar-relativistic tight binding LMTO calculation. On the experimental side, Cotti et al. [6] have reported measurements of the

photoemission spectrum of liquid mercury. On the basis of photoemission work, Oellhafen et al. [7] have also pointed to the existence of a minimum in the DOS at the Fermi level in liquid mercury. Yao [8] has reported electronic properties of expanded mercury using optical absorption spectra.

Within the last three decades, Compton scattering has emerged as a powerful tool for the investigation of the behaviour of valence electrons [9]. The Compton profile (CP), $J(p_z)$, can also be directly interpreted in terms of the ground state momentum distribution $\rho(\mathbf{p})$ of the target, i. e.

$$J(p_z) = \iint \rho(\vec{\mathbf{p}}) dp_x dp_y. \quad (1.1)$$

In this paper we report first the experimental Compton profile of liquid Hg, measured at room temperature. In addition to usual data corrections, we have included for the first time a new back ground correction owing to bremsstrahlung radiation generated in such experiments.

We have decided to measure the CP of liquid Hg for two reasons: (a) non-availability of theoretical directionally–dependent Compton profiles of Hg, and (b) difficulty in growing, handling and orienting single crystals of mercury.

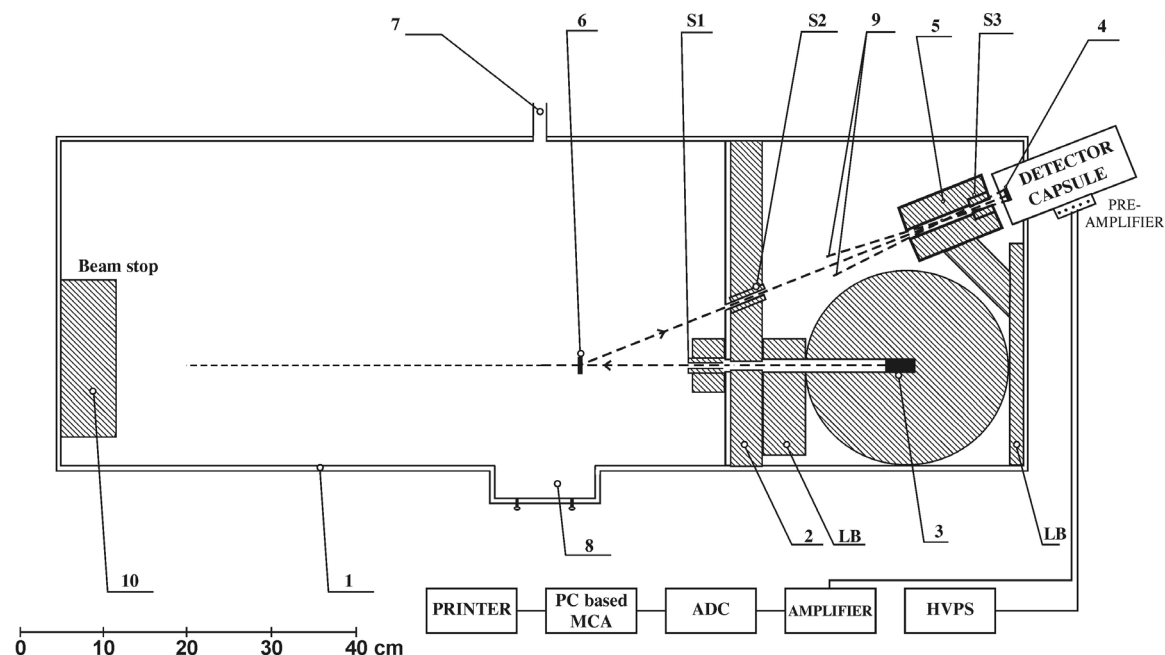


Fig. 1. Layout of ^{137}Cs Compton spectrometer shown here are: Steel chamber 115 cm · 35 cm · 40 cm (1), lead partition (2), ^{137}Cs source (3), HPGe detector crystal (4), detector collimation (5), sample (6), port for evacuation (7), additional window for 90° scattering (8), volume seen by detector (9), beam stop (10), collimating slits (S1 to S3) and lead bricks (LB). Other shaded regions also shows the lead shielding. The lead shielding (5–7 cm) all around the steel chamber is not shown here.

Since the renormalised-free-atom (RFA) model is known to be a reasonable compromise between band structure and simple atomic calculations, we have also attempted to interpret our experimental data in terms of RFA and free-electron models.

2. Experiment

The details of the Compton spectrometer (as shown in Fig. 1) are published in [10]. The performance of the spectrometer was tested using well-explored standard samples like Al, Ta. The Compton profiles of the standard samples were found to agree very well with the reported experimental and theoretical data. The salient features of the experimental set-up are: The Compton spectrometer is based on a 20 Ci ^{137}Cs source, which emits photons of 661.65 keV. The sample (liquid Hg) was kept in an ampoule having a bulk thickness of 3 mm and mylar windows. The distance between source and sample was 380 mm. The incident beam, scattered inelastically on the sample through $160^\circ (\pm 0.7^\circ)$, was detected by a high purity planar Ge detector (Canberra GLP0210P), 548 mm distant from the sample. The channel width of the multi-

channel analyser (Genie2000, Canberra) was approximately 0.035 a.u. on the electron momentum scale (1 a.u. of momentum = $1.993 \cdot 10^{-24}$ kg ms $^{-1}$), and the overall momentum resolution of the spectrometer was 0.38 a.u., which is much better than for conventional ^{241}Am based Compton spectrometers (0.6 a.u.). An integrated Compton intensity of 13 million photons was obtained during the measuring time of about 15 days. Figure 2 shows the raw data of the Compton profile of Hg. During the measurement, the stability of the system was checked several times, using weak ^{57}Co and ^{133}Ba calibration sources. The background was measured by running the system with empty ampoule for a period of about 4 days, and was then subtracted from the raw-data point-by-point after scaling it to the counting time of the sample. Thereafter, the profile was corrected for the effects of detector response function, energy dependent detector efficiency, absorption and scattering cross-section, following the data correction package of the Warwick group [11]. The correction of the detector response function was restricted to stripping the low energy tail off the resolution function and smoothing the data leaving the theory to be convoluted with a Gaussian of 0.38 a.u. (full width at half maxi-

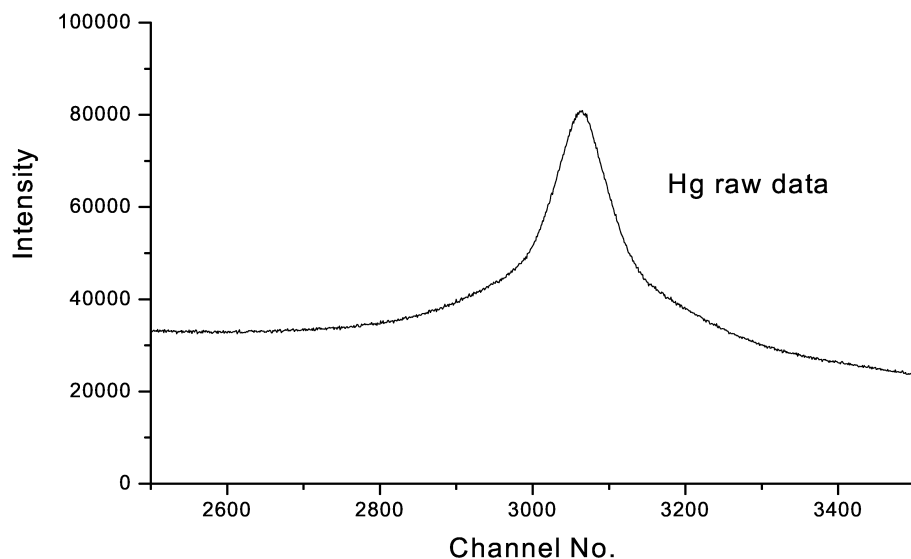


Fig. 2. Energy distribution of 661.65 keV photon from a ^{137}Cs source scattered at $160^\circ (\pm 0.7^\circ)$ from liquid mercury. Each channel corresponds to about 63 eV (0.035 a.u. of momentum).

mum). After converting the profile into the momentum scale, a Monte Carlo simulation [12] of the multiple scattering was performed. The percentage of multiple scattering in the final profile (-10 a.u. to $+10$ a.u.) was 10.6%, which increases the $J(0)$ value by 4.62%. Thereafter, the profile was corrected for the additional background correction due to bremsstrahlung radiation, as discussed later on.

Finally the experimental profile for Hg was normalized to have the area of 28.73 electrons being the area of the free atom profile in the momentum range of 0 to $+7$ a.u. [13].

3. Calculations

a) Renormalized Free Atom (RFA) Model

In absence of band structure Compton profile calculations, the profile was computed using the RFA model [14, 15], which was found to be a reasonable choice in case of 4d and 5d transition metals, see, for example [16–19]. The free-atom Hartree-Fock (HF) wave function for 6s electrons in Hg were taken from the table of Hermann and Skillman [20]. The wave function was truncated at the Wigner-Seitz (WS) radius (3.34 a.u.) and normalized to unity to preserve charge neutrality. It turned out that only about 66% of the 6s wave functions was contained in the WS sphere. For the 5d wave function the corresponding number was about 99%. Therefore, the Compton profile $J_{6s}(p_z)$ due to only 6s electrons (where the wave function was

quite extended) was computed as

$$J_{6s}(p_z) = 4\pi \sum |\Phi_o^c(K_n)|^2 G_n(p_z), \quad (3.1)$$

where $\Phi_o^c(K_n)$ is the Fourier transform of the RFA wave function and $G_n(p_z)$ is an auxiliary function involving reciprocal lattice vectors (K_n), number of points in the n^{th} shell in reciprocal space, Fermi momentum p_F , etc. To incorporate the crystalline effect, 25 shortest reciprocal lattice vectors were taken into account to compute the $J_{6s}(p_z)$. It is worth mentioning that the isotropic Compton profile is almost independent of the structure, the determining factor being the average electron density, as mentioned by Ahuja *et al.* [21]. It is supported by the work of Papanicolaou *et al.* [22], who assumed the hcp Zr to be a fcc metal to calculate the isotropic Compton profile. In our RFA calculations we have assumed the structure of Hg as fcc: which in fact is a distorted fcc structure.

b) Free Electron Calculation

The free electron Compton profile was obtained for 6s electrons within the framework of free electron model [15] using the formulae

$$J_{6s}(p_z) = \begin{cases} 3n(p_F^2 - p_z^2)/4p_F^3 & \text{for } p_z \leq p_F, \\ 0 & \text{for } p_z > p_F. \end{cases} \quad (3.2)$$

In case of Hg, the number of free electrons (n) was taken as 2.

For both model calculations, the contribution of core electrons and also the outermost d electrons was di-

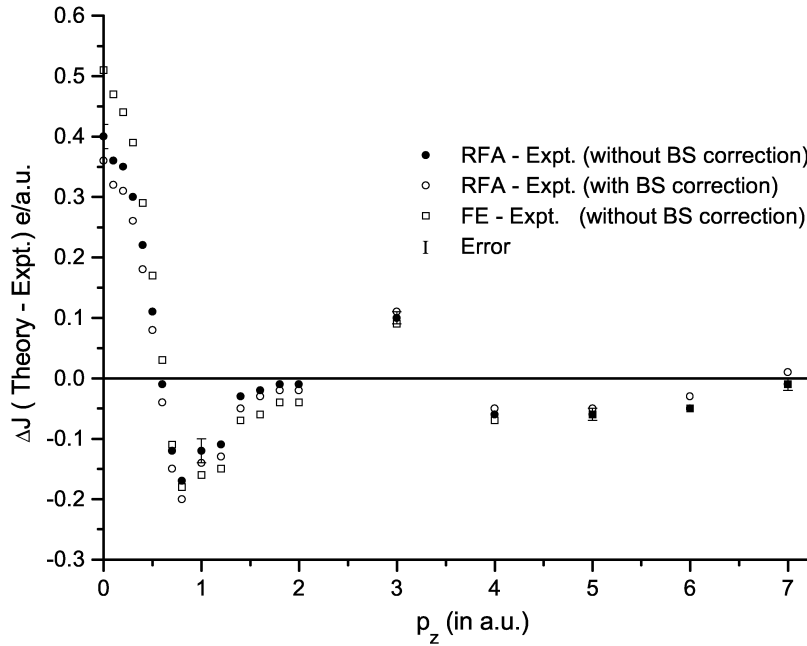


Fig. 3. A plot of the difference between the convoluted RFA model and experiment (a) without bremsstrahlung correction, (b) with bremsstrahlung correction. Difference between the convoluted free electron and without bremsstrahlung is also shown. The statistical errors ($\pm\sigma$) are shown for few points.

rectly taken from the tables of Biggs *et al.* [13] and was added to these valence profiles. The total theoretical profiles (0–7 a.u.) so obtained were normalized to 28.73 electrons as the experimental ones.

4. Results and Discussion

In Table 1 we present the experimental Compton profile of Hg together with the unconvoluted RFA for $4f^{14}5d^{10}6s^2$ configuration and free-electron profiles. For actual comparison of experiment with theory (columns 2, 3), the theoretical profiles were convoluted with a Gaussian of FWHM 0.38 a.u. The difference profiles ΔJ (convoluted theory minus experiment without bremsstrahlung background correction) are depicted in Figure 3. It can be seen that near $J(0)$, both the theoretical profiles are higher than the experimental ones, while a reverse trend is seen in the momentum range 0.7 to 2.0 a.u. Near 3 a.u. the theory becomes higher than the experiment, as can be seen from the Table 1 and Figure 3. It is obvious that there are small deviations in the high momentum regime (5 to 7 a.u.), in which the contribution from the valence electrons is almost negligible. Such deviations were also seen in the Compton study of some 4d/5d metals (see, for example, [21] and [23]). Some of the possible causes may be the continuous spectrum of bremsstrahlung (BS) emitted by photo and Compton

Table 1. Theoretical (unconvoluted) and experimental isotropic Compton profiles of liquid Hg, measured at room temperature. All quantities are in atomic units (a. u.). The statistical errors ($\pm\sigma$) are sometimes shown.

p_z	$J(p_z)$ in e/a.u.				
	RFA $4f^{14}5d^{10}6s^2$	Free electron	Expt. (without BS)	Expt. (with BS)	Bremsstrahlung profile
0	10.19	10.29	9.72 ± 0.02	9.76 ± 0.02	0.031
0.1	10.10	10.21	9.66	9.70	0.031
0.2	10.07	10.16	9.54	9.58	0.031
0.3	9.77	9.89	9.37	9.41	0.031
0.4	9.52	9.57	9.15	9.19	0.031
0.5	9.06	9.16	8.89	8.92	0.031
0.6	8.64	8.64	8.61	8.64	0.031
0.7	7.95	8.02	8.34	8.37	0.031
0.8	7.79	7.74	8.06	8.09	0.031
1.0	7.41	7.37	7.51 ± 0.02	7.53 ± 0.02	0.031
1.2	6.93	6.89	7.02	7.04	0.031
1.4	6.40	6.36	6.43	6.45	0.031
1.6	5.86	5.82	5.89	5.90	0.031
1.8	5.34	5.31	5.37	5.38	0.031
2.0	4.87	4.85	4.91	4.92	0.031
3.0	3.44	3.44	3.36 ± 0.01	3.35 ± 0.01	0.031
4.0	2.85	2.84	2.91	2.90	0.030
5.0	2.38	2.38	2.44 ± 0.01	2.43 ± 0.01	0.030
6.0	1.93	1.93	1.98	1.96	0.030
7.0	1.56	1.56	1.59 ± 0.01	1.57 ± 0.01	0.030

electrons and the low energy tail in the primary radiation due to self scattering within the source.

In this section, we also discuss the contribution of BS, which was not explored properly for 661.65 keV ^{137}Cs Compton scattering experiments. It is well established that the photo and Compton electrons ejected during the interaction process produce BS under the

influence of atomic nuclei. These BS photons also contribute in the measured Compton profiles [24, 25]. We have estimated the total contribution of these BS photons due to both photoelectric and Compton

effects. For the computation of the BS intensity we have used the prescription of Koch and Motz [26]. Accordingly, the differential BS cross-section (within relativistic Born approximation) for the emission of a photon with energy w is given by

$$\frac{\partial \Phi_w}{\partial w} = \frac{\Phi}{w} \frac{p}{p_0} \left\{ \frac{4}{3} - 2E_0E \left(\frac{p^2 + p_0^2}{p^2 p_0^2} \right) + \frac{\varepsilon_0 E}{p_0^3} + \frac{\varepsilon E_0}{p^3} - \frac{\varepsilon \varepsilon_0}{p_0 p} \right. \\ \left. + L \left[\frac{8E_0E}{3p_0 p} + \frac{w^2(E_0^2 E^2 + p_0^2 p^2)}{p_0^3 p^3} + \frac{w}{2p_0 p} \left(\left(\frac{E_0 E + p_0^2}{p_0^3} \right) \varepsilon_0 - \left(\frac{E_0 E + p^2}{p^3} \right) \varepsilon + \frac{2wE_0E}{p^2 p_0^2} \right) \right] \right\}, \quad (4.1)$$

where

$$L = 2 \ln \left[\frac{E_0 E + p_0 p - 1}{w} \right], \quad \varepsilon_0 = \ln \left(\frac{E_0 + p_0}{E_0 - p_0} \right), \quad \varepsilon = \ln \left(\frac{E + p}{E - p} \right), \quad \text{and } \Phi_0 = Z^2 \cdot 5.78 \cdot 10^{-28} \text{ cm.}$$

Here E_0 and E are the initial and final total energy of the electron in a collision, in $m_0 c^2$ units; p_0 and p are the initial and final momentum of the e^- in a collision in $m_0 c$ units; w is the energy of the emitted photon in $m_0 c^2$ units, Z is the atomic number of the target material. It is to be noted that the initial kinetic energy of Compton electrons is obtained by considering the average energy of the Compton scattered photons as 189 keV (Compton peak). We define RD^P as the relative differential BS contribution due to photoelectrons from all the shells of the Hg atom, and RD^C as that due to Compton electrons.

Then,

$$RD^P = \left[\frac{w}{E_0} \sum_i \sigma_{pe,i} \left(\frac{d\Phi}{dw} \right)_i \right] \\ \text{and } RD^C = \frac{w}{E_0} \sigma_C \left(\frac{d\Phi}{dw} \right) \quad (4.2)$$

(σ corresponds to respective cross-sections).

The total BS intensity (Φ_w) due to photo and Compton electrons, can be written as

$$\Phi_w = \Phi_{wp} + \Phi_{wc}, \quad (4.3)$$

where

$$\Phi_{wp} = \int_0^{T_0} (RD^P) dw, \quad \Phi_{wc} = \int_0^{T_0} (RD^C) dw.$$

T_0 is the initial kinetic energy of the electrons in $m_0 c^2$ units.

The spectral distribution of Φ_w for liquid Hg (at 661.65 keV incident energy) for photon energies in

the range 1 keV to 660 keV is shown in Figure 4. We have used this plot to find the ratio $I_{BS}^C / I_{BS}^{\text{total}}$ (i.e. the intensity of BS in the Compton region relative to the total BS intensity). For this, we calculated (from Fig. 4) the ratio of areas of total BS cross-section (Φ_w) in the Compton energy range (176 keV to 202 keV: corresponds to -7 a.u. to $+7$ a.u.) and the total energy range. This ratio came out to be 0.0527. Further, the ratio $I_{BS}^{\text{total}} / I_C^{\text{total}}$ (where I_C^{total} is the total intensity of the Compton radiation) for liquid Hg was obtained using the relations given in [25, 27], which was found to be equal to 0.1447. Thus, the ratio of the total BS intensity in the Compton region (I_{BS}^C) to the total Compton Intensity (I_C^{total}) was obtained by taking the product of the above two ratios. It was found to be equal to 0.0076. This product was then multiplied by the number of electrons in the Compton region -7 a.u. to $+7$ a.u. viz. 57.46 to get the area under the curve of the BS profile. It was calculated to be equal to 0.44 e. Therefore, the area under the BS curve in the Compton region (-7 to $+7$ a.u.) of Fig. 4 was normalized to 0.44 e to get the data of the BS profile in e/a.u. units. This corresponds to an additional BS background contribution. After subtracting the BS profile point by point from the duly corrected experimental profile (column 4), the BS corrected profile was again normalized to the total area of free atom profile viz. 28.73 e in the range 0 to $+7$ a.u. The duly normalized profile after BS correction and BS background profile are also given in column 5 and 6 of Table 1.

Coming back to Fig. 3, it can also be seen that, even after BS correction, in the low momentum region (0–0.6 a.u.), the theoretical values are higher than the ex-

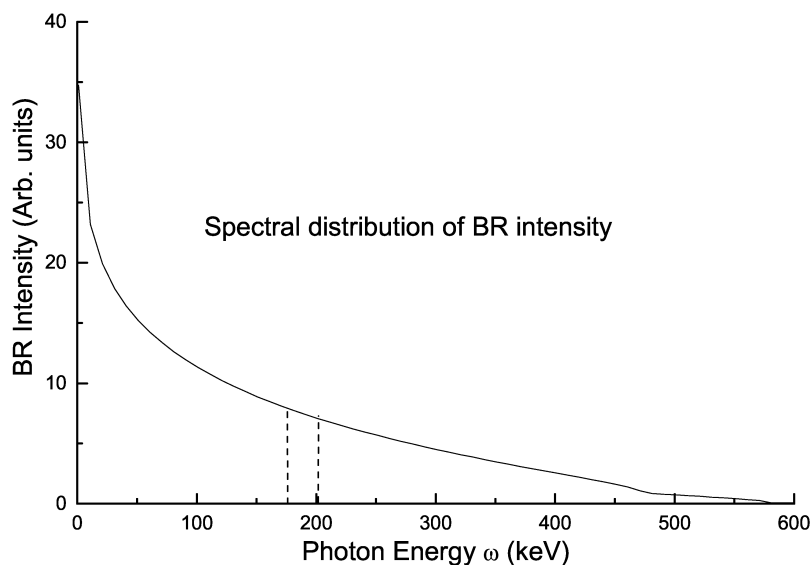


Fig. 4. Spectral distribution of bremsstrahlung calculated for decelerating electrons liberated in photoelectric and Compton processes resulting from 661.65 keV γ -rays in mercury (for the calculation see the result and discussion part). Vertical dotted lines show the Compton region.

perimental ones. This may be due to s-p hybridization in the valence states of mercury. Our experience in this field guides us that the Compton profile corresponding to 6p electrons of Hg is supposed to be flatter than the 6s electrons. Hence incorporation of 6p electrons in theoretical calculations will decrease the magnitude of the total theoretical profiles in this region which will lead to a good agreement between theory and experiment. Since 6p electron wave functions are not available in the literature, it is not possible to consider these electrons within the RFA scheme. The poor agreement between experiment and the free electron Compton profile (even after BS correction: not shown here) shows the inapplicability of the free electron model for liquid mercury. The s-p hybridization suggests a 'covalent like' character of liquid (rhombohedral) mercury, which agrees with the LMTO calculation of Bose [5] and the scalar-self consistent calculation of Singh [28].

5. Conclusions

The observed discrepancies between the experimental and theoretical data (RFA and free electron)

illustrate the inadequacy of these calculations to model the electron momentum density in Hg. Our measurements support s-p hybridization which agrees with LMTO and scalar-relativistic results. Fully relativistic band structure calculations of the electron momentum density and Compton profiles of Hg are required for a quantitative interpretation of the data.

Acknowledgement

This work is partially supported by a grant from Department of Science and Technology (DST), New Delhi vide grant No. SP/S-2/M03/99. We thank Prof. B. K. Sharma, Univ. of Raj., Jaipur; Dr. E. Zukowski and A. Andrejczuk, Warsaw University, Poland; Dr. B. K. Godwal, BARC, Mumbai and Mr. A. Khan, M. L. Sukhadia University for their valuable help in setting-up the 20 Ci ^{137}Cs Compton spectrometer. One of us (BLA) is thankful to Prof. M. J. Cooper, Univ. of Warwick, U. K. for a discussion about Compton spectroscopy using ^{137}Cs gamma-rays.

- [1] A. P. Cracknell, *The Fermi surfaces of metals*, Taylor and Francis, London 1971.
- [2] L. E. Ballentine, *Adv. Chem. Phys.* **31**, 263 (1975).
- [3] G. Kresse and J. Hafner, *Phys. Rev.* **B 55**, 7539 (1997).
- [4] W. Jank and J. Hafner, *Phys. Rev.* **B 42**, 6926 (1990); also W. Jank and J. Hafner, *J. Non-Cryst. Solids* **117/118**, 304 (1990).
- [5] S. K. Bose, *J. Phys.: Condens. Matter* **11**, 4597 (1999).
- [6] P. Cotti, H.-J. Guntherodt, P. Munz, P. Oellhafen, and J. Wullschlegler, *Solid State Commun.* **12**, 635 (1973).
- [7] P. Oellhafen, G. Indlekofer, and H.-J. Guntherodt, *Z. Phys. Chem.* **NF 157**, 483 (1988).
- [8] M. Yao, *Z. Phys. Chem. (Germany)* **184**, 73 (1994).
- [9] M. J. Cooper, *Rep. Prog. Phys.* **48**, 415 (1985).

- [10] B. L. Ahuja and M. Sharma, *Solid State Physics (India)* Vol. **46** (2004) Conference Proceedings – In press; also B. L. Ahuja and M. Sharma, To be communicated (2004).
- [11] See, for example, D. N. Timms, Ph.D. Thesis (unpublished), University of Warwick, England (1989); also B. G. Williams, *Compton scattering*, McGraw-Hill, London (1977).
- [12] J. Felsteiner, P. Pattison, and M. J. Cooper, *Phil. Mag.* **30**, 537 (1974).
- [13] F. Biggs, L. B. Mendelsohn, and J. B. Mann, *At. Nucl. Data Tables* **16**, 201 (1971).
- [14] K. F. Berggren, *Phys. Rev.* **B6**, 2156 (1972).
- [15] B. L. Ahuja, B. K. Sharma, and O. Aikala, *Pramana – J. Phys (India)* **29**, 313 (1987).
- [16] B. K. Sharma and B. L. Ahuja, *Phys. Rev.* **B38**, 3148 (1988).
- [17] Usha Mittal, B. K. Sharma, Farid M. Mohammad, and B. L. Ahuja, *Phys. Rev.* **B38**, 12208 (1988).
- [18] B. K. Sharma, M. D. Sharma, K. B. Joshi, B. L. Ahuja, and R. K. Pandya, *Phys. Stat. Sol. (b)* **196**, 347 (1996).
- [19] K. B. Joshi, R. K. Pandya, B. L. Ahuja, and B. K. Sharma, *Pramana – J. Phys (India)* **48**, 1105 (1997).
- [20] F. Hermann and S. Skillman, *Atomic structure calculations*, Prentice-Hall Inc., Englewood, Cliff (N.J.) 1963.
- [21] B. L. Ahuja, M. D. Sharma, B. K. Sharma, S. Hamouda, and M. J. Cooper, *Physica Scripta* **50**, 301 (1994).
- [22] N. I. Papanicolaou, N. C. Bacalis, and D. A. Papaconstantopoulos, *Phys. Rev.* **B37**, 8627 (1988).
- [23] R. K. Pandya, K. B. Joshi, R. Jain, B. L. Ahuja, and B. K. Sharma, *Phys. Stat. Sol. (b)* **200**, 137 (1997).
- [24] N. G. Alexandropoulos, T. Chatzigeorgiou, G. Evangelakis, M. J. Cooper, and S. Manninen, *Nucl. Instrum. Method A* **271**, 543 (1988).
- [25] U. Mittal, B. K. Sharma, R. K. Kothari, and B. L. Ahuja, *Z. Naturforsch.* **48a**, 348 (1993).
- [26] H. W. Koch and J. W. Motz, *Rev. Mod. Phys.* **31**, 920 (1959).
- [27] R. D. Evans, *The Atomic Nucleus*, Tata McGraw-Hill, New Delhi 1979.
- [28] P. P. Singh, *Phys. Rev. Lett.* **72**, 2446 (1994).